Eur. J. Med. Chem. 33 (1998) 451–462

Evidence for new non-steroidal human aromatase inhibitors and comparison with equine aromatase inhibition for an understanding of the mammalian active site

Pierrick Auvray[a,1], Safa Moslemi[a], Pascal Sourdaine[a], Sébastien Galopin[a], Gilles-Eric Séralini[a]*, Cécile Enguehard[b,1], Patrick Dallemagne[b], Ronan Bureau[b], Pascal Sonnet[b], Sylvain Rault[b]

[a]*EP CNRS 9, IBBA, Laboratoire de Biochimie et Biologie Moléculaire, Université de Caen, Esplanade de la Paix, 14032 Caen Cedex, France*
[b]*C.E.R.M.N., Laboratoire de Pharmacochimie, 1, rue Vaubénard, 14032 Caen Cedex, France*

(Received 16 October 1997; accepted 28 January 1998)

Abstract – We developed a new comparative model in order to better understand the structure–function relationships of the active site in human aromatase. Thus, we undertook the comparative inhibition of human and equine aromatases with new compounds. In fact, equine aromatase represents the only easy and available mammalian membrane-bound enzyme model, besides the human one, which is biochemically purified, well characterized and cloned. During the course of our work concerning the synthesis and screening of new drugs on human and equine aromatases, we identified two new indane derivatives which inhibited the human enzyme (IC_{50} = 3.5 μM and 5.9 μM) strongly and selectively while they were much less active on the equine one (IC_{50} > 10 μM). The hitherto known aromatase inhibitors, such as 4-hydroxyandrostenedione (4-OHA) and some other indane-related derivatives, are equally efficient on both human and equine enzymes. In this work, using a theoretical 3D model of aromatase, we have explained the human selectivity of the new described compounds as due to the specific differences between the primary structure of both active sites in human and equine enzymes. These results could allow synthesis of a new family of compounds that are much more potent and selective aromatase inhibitors. © Elsevier, Paris

aromatase inhibitor / structure–function relationship / indane derivative / breast cancer / horse

1. Introduction

The aromatase enzyme complex, responsible for the conversion of androgen to estrogen, is formed by the specific cytochrome P450 aromatase ($P450_{arom}$) and an ubiquitous flavoprotein NADPH cytochrome P450 reductase. It is involved in reproduction, development, sexual differentiation and behaviour, in some brain functions, as well as in the growth of hormone-dependent cancers [1]. In the search for new leads for inhibition of estrogen biosynthesis by $P450_{arom}$, 2-aryl-methylenindan-1-ones have recently been evaluated with regard to this enzyme [2, 3]. This is important for the treatment of some breast cancers. Today, a lot of inhibitors have already been studied [4]. The first and second generation of aromatase inhibitors, like the nonsteroidal aminoglutethimide [5] and the steroidal substrate analogue 4-OHA [6], are presently the major clinically available inhibitors. However, a third generation of potent non-steroidal aromatase inhibitors have been developed more recently including letrozole, vorozole and anastrozole [7, 8, 9]. But, because of the results obtained in vivo, the need for clinical drugs with increased specificity, clinical efficiency and tolerability remains a challenge in the development of new compounds [10, 11]. Improvement of new drugs may be realized by screening of molecules derived from already known inhibitors or natural substrates of aromatase, but also with greater precision by taking into consideration our understanding of the enzyme structure. Actually, the model of the human membrane-bound aromatase has been deduced from comparative sequence homology studies with identified structures of soluble bacterial cytochrome P450 which have been crystallized [12–14]. These comparisons show only 17% identity between $P450_{arom}$ and P450BM3 [15]. The active site was also studied by site-directed mutagenesis coupled with

*Correspondence and reprints
[1]P.A. and C.E. have equally contributed to this work and should both be considered as first authors.

analysis of the binding characteristics of human aromatase inhibitors [15]. To increase our knowledge of the aromatase structure and consequently to obtain improved inhibitors, it is crucial that new comparative models be developed. Thus, we have used equine testicular aromatase which presents 78% primary structure identity with the human enzyme [16]. This enzyme, responsible for elevated estrogen concentrations in the adult stallion, is the only easy and available mammalian membrane-bound model, besides the human one, which is biochemically purified, well characterized and cloned [16–23]. Biochemically, it presents very good similarities with the human enzyme, but also some noticeable differences such as 19-norandrogens aromatization [24]. Moreover, when comparing the primary structure of both enzymes, it appeared that there were only a few crucial non-conservative changes in the active site domain [16] which may be responsible for their enzymatic specificities. The aim of this work was to screen new indane derivatives with human placental aromatase and to compare their potencies with the equine testicular one. By taking into account data from both models, it may be possible to provide further details concerning the model of the mammalian active site; this will in turn clarify the design of the new inhibitors.

2. Chemistry

We previously described the one-pot synthesis of methoxy-3-trifluoroacetylaminoindan-1-ones **7–9** starting from methoxybenzaldehydes **1–3** via 3-amino-3-(methoxyphenyl)propionic acids **4–6** by means of refluxing in trifluoroacetic acid and its anhydride [25] (*figure 1*).

Treatment of an ethanolic solution of **7**, **8** or **9** with a 5 N aqueous sodium hydroxide solution gave a mixture to which was then added 1.5 equivalent of arylcarboxaldehyde (*figure 2*). After stirring for 2 h at room temperature, 2-arylmethylene-3-trifluoroacetyl aminoindan-1-ones **10–16** were precipitated from the reaction mixture by addition of dilute aqueous hydrochloric solution.

The *E*-configuration of **10–16** was determined by ^{1}H-NMR analysis which exhibited vinyl-H singlets between 7.49 and 7.61 ppm, in accordance with the literature [26] and with the deshielding effect of the indane carbonyl group. In order to prove this configuration, we carried out partial isomerization of **14**-(*E*) into **14**-(*Z*) by UV irradiation according to a method (*figure 3*) previously reported [3]. ^{1}H-NMR analysis of the mixture showed a shielded vinyl-H singlet at 7.06 ppm for the *Z*-form (7.61 ppm for the corresponding *E*-form).

Alkaline hydrolysis of the trifluoroacetamido group of **10–16** did not take place and only led to degradation products. However, by prolonging reaction for 24 h the aldol condensation of **7–9** with an arylcarboxaldehyde, free bases **17–21** were precipitated from the reaction mixture by addition of water.

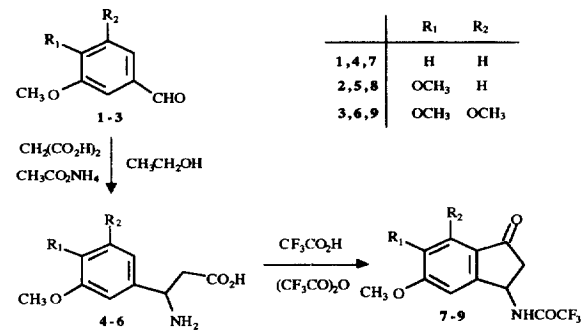

	R_1	R_2
1,4,7	H	H
2,5,8	OCH_3	H
3,6,9	OCH_3	OCH_3

Figure 1. Synthesis of compounds **7–9**.

The ^{1}H–^{1}H COSY–NMR spectra of **17–21** did not exhibit either vinyl-H or H-3 signals but a CH_2 signal between 3.45 and 3.61 ppm. These data were in favor of the rearranged 3-amino-2-arylmethylinden-1-ones **17–21** in which the exo double bond migrated inside the indane ring.

3. Biological results on human aromatase

We have screened twelve newly synthesized indane derivatives for their human aromatase inhibitory activities (numbered 10–21, *figure 2*). We evidenced two molecules, **19** (MR 20814) and **21** (MR 20818), that show an 82% inhibition of aromatase activity at 15 μM (*figure 4A*). This is comparable to the effect of compound **22** [3]. The IC_{50} values (*table I*) with human aromatase are equivalent between compounds **19**, **21** and **22**: 3.5 ± 1.2 μM, 5.9 ± 0.7 μM and 5.2 ± 2.7 μM, respectively. These values are in the same order of magnitude as for 4-OHA (0.5 ± 0.3 μM), known as a specific steroidal aromatase inhibitor. All these IC_{50} values evidence inhibitory potencies 20–50 times greater than aminoglutethimide [5]. But in comparison letrozole, vorozole and anastrozole are respectively around 200, 1000, and 5000 times more potent inhibitors [7–9]. However, the best IC_{50} does not always correspond to the best specific inhibition in vivo [11]. Moreover, results reported on *figure 5* show that the indane derivatives, as well as 4-OHA, presented a competitive inhibition. Corresponding K_i values are summarized in *table II*. The K_i/K_m ratio values, which represent the relative inhibition potency for an inhibitor, were evaluated (*table II*). They reveal

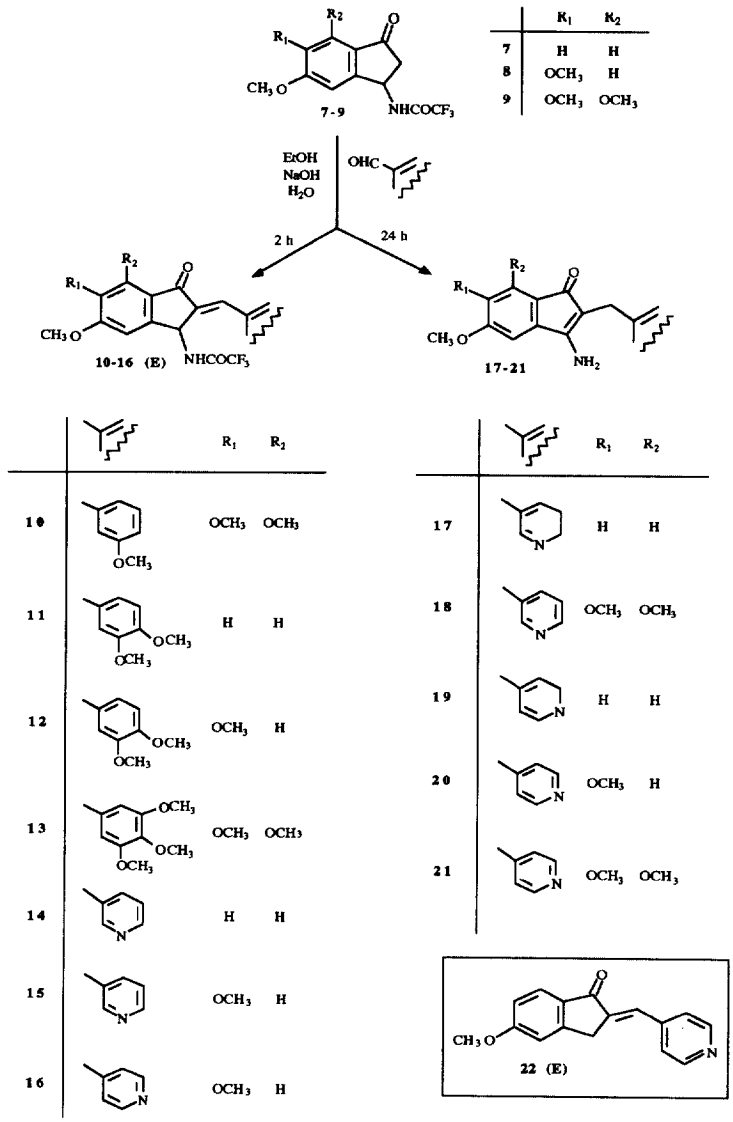

Figure 2. Different compounds used in this study.

that compounds **19** and **21** are quite potent inhibitors for human aromatase (K_i/K_m of 6.7 ± 0.6 and 17.0 ± 2.2 with **19** and **21** respectively), in the same order of magnitude as for 4-OHA (1.6 ± 0.7) and compound **22** (6.9 ± 0.4). In order to better understand the mechanism of this inhibition, we have studied the inactivation of this enzyme by compounds **19**, **21** and **22** in comparison to 4-OHA which is known to be an inactivator [27]. *Figure 6* shows that indane derivatives are not inactivators and that these compounds did not exhibit a covalent-type interaction with the active site. The interaction between a cytochrome P450 and its substrate can be further characterized by spectral studies [28]. A type II-spectrum, with minimal absorbance at 390 nm and maximal absorbance at 420 nm, is considered as specific for an interaction between a nitrogen atom of the molecule and the heme iron of the cytochrome, whereas a type I-spectrum (inverted absorbance for 4-OHA for instance [28]) is observed when this type of interaction is absent. All the tested

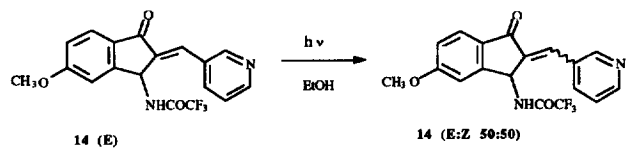

Figure 3. Partial isomerization of compound **14**-(*E*) into **14**-(*Z*).

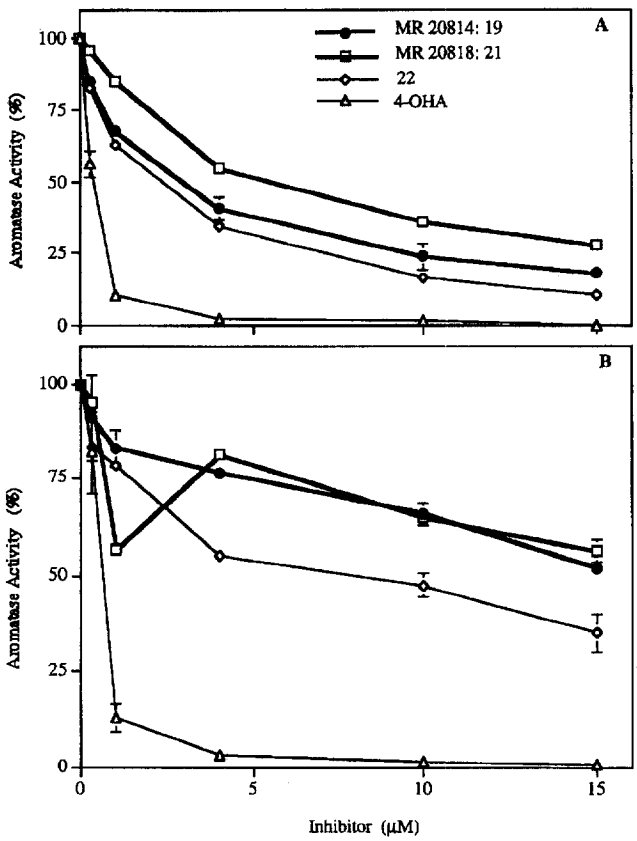

Figure 4. Inhibitions of human (A) and equine (B) aromatases by compounds **19** and **21** in comparison with 4-OHA and **22**. Aromatase activity in microsomes was evaluated by measuring ^3H_2O released from 200 nM [1β, 2β-^{3}H] androstenedione at 37 °C during 15 min, in the presence of inhibitors **19** and **21** and of controls **22** and 4-OHA. The concentrations used ranged from 0 to 15 μM. The inhibition of aromatase in human placental (16 μg) and equine testicular microsomes (20 μg) was performed in the presence of 60 μM NADPH,H+. Blank was realized without adding NADPH,H+. The results are expressed as % to a standard control which was incubated with NADPH,H+ and without inhibitor, and are the mean of triplicate values ± SD; SD is sometimes not visible at the scale.

Table I. Aromatase inhibition with different indane derivatives used in this study. Compounds **10–18** and **20**, not indicated in this table, did not show inhibition at the highest concentration tested (15 μM). 4-OHA values are given for comparison.

Compound	IC_{50} (μM)	
	Human aromatase	Equine aromatase
19	3.5 ± 1.2	> 10
21	5.9 ± 0.7	> 10
22	5.2 ± 2.7	7.3 ± 1.8
4-OHA	0.5 ± 0.3	0.6 ± 0.3

compounds **19**, **21** and **22** show a type II-spectrum with the human aromatase (*figure 7* and data not shown). A molecular modelling study was also carried out to compare the 3D structure of **19** and **22** (3D structure of **21** was similar to **19**, see below).

4. Biological results on equine aromatase

In order to better understand the active site of the human aromatase by comparing it to other species, we have tested the indane derivatives on the equine enzyme (*figure 4B*). The IC_{50} values (*table I*) observed with the same compounds are relatively different from the human one (> 10 μM for **19** and **21**), except with compound **22** and 4-OHA which are in the same range (7.3 ± 1.8 μM and 0.6 ± 0.3 μM respectively). Such differences, with inhibitors observed with two very comparable mammalian enzymes, suggest conformational differences in their active sites. Furthermore, although compounds **19** and **21** presented a competitive inhibition (*figure 8*), they are weak inhibitors of equine aromatase as was reflected by their high K_i/K_m ratio values (100.0 ± 6.4 and 93.4 ± 9.3 for **19** and **21** respectively) whereas the ratio values observed for compound **22** (20.9 ± 0.4) and 4-OHA (1.1 ± 0.0) are similar to those obtained with the human enzyme (*table II*). All our results taken together show that the affinities of our compounds are different for the two enzymes and indicate that some of these molecules interact differently with the active site. Finally, our results concerning the specific differences between these two mammalian aromatases were reinforced by the differential interaction between **19** and equine aromatase which was characterized by a type I-spectrum (*figure 7*) in contrast to the type II-spectrum observed with the human one. These results verified

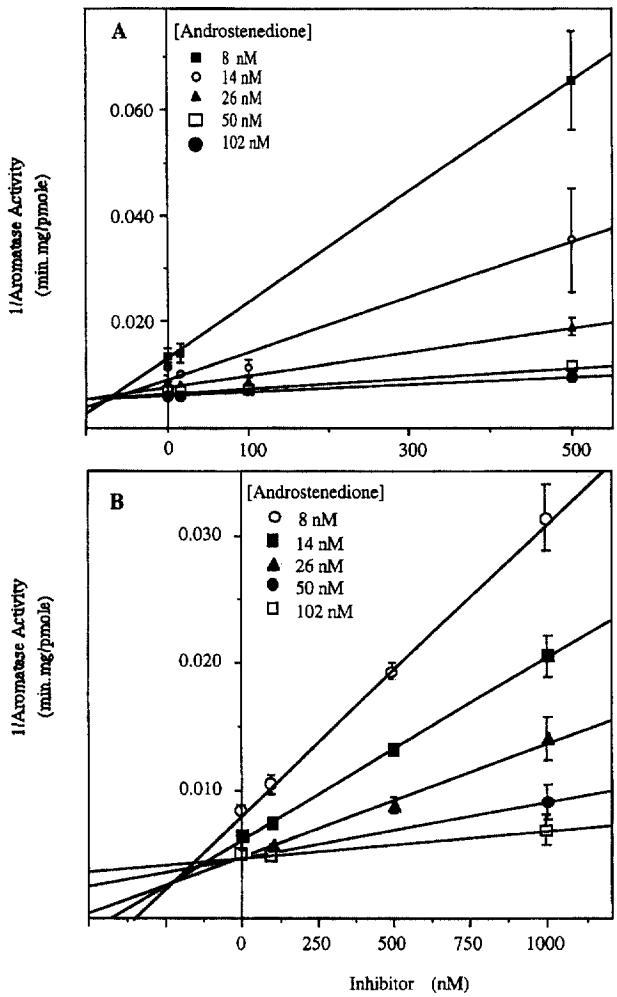

Figure 5. Kinetic inhibition studies with compounds **19** (A) and **21** (B) on human aromatase. Aromatase activity was evaluated by incubating 4 µg placental microsomes with [1β,2β-^{3}H] androstenedione (8–102 nM) and with 0 to 500 nM compound **19** (A) or 0 to 1000 nM compound **21** (B) at 37 °C during 10 min. K_i were determined graphically by using Dixon-plots. Results are expressed as pmol estrogen formed/min•mg microsomal proteins and are the mean of triplicate values ± SD.

our hypothesis concerning a differential position of **19** inside the active site between human and equine aromatases. This outcome could be explained by primary structural differences of both active sites which could be responsible for biochemical specificities of human and equine aromatases [29]. Keeping these data in mind, a 3D molecular model of human aromatase was built to see if the known model could provide an explanation for these results.

5. Examination of a 3D model for compound 19 and for the $P450_{arom}$ active site

Compound **19** was built with standard bond lengths and angles using the program UNICHEM version 3.0 (Cray research) and a molecular dynamic calculation was carried out. We were particulary interested by the evolution of the distance in compound 19 between the nitrogen of the pyridin group and the oxygen of the keto group or the nitrogen of the amino group during the simulation (*figures 9* and *10*). The average distance during the simulation between the oxygen and the nitrogen of the pyridin group was 6.4 Å with a standard deviation of 0.51 Å. This distance was close (*figure 11* for one conformer), for several conformers, to the distance between these two atoms for **22** (7.2 Å for the *E*-isomer). The first observation could explain the pharmacological result which shows the identical affinities of **19** and **22** towards human aromatase (*figure 4A* and *table II*).

For the distance between the two nitrogens, the average was 5.4 Å with a standard deviation of 0.56 Å. The function of the nitrogen group could not be explained wih these first results. However, a molecular modelling study previously carried out on 3-alkyl-3(4-pyridyl)piperidine-2,6-dione [30] enabled us to make an hypothesis. With these compounds, a distance between the two nitrogens of 5.4 Å, for the *R*-isomer, was observed. Moreover, in this study, the alkylation at the glutarimide nitrogen led to derivatives whose aromatase inhibitory activity increased with chain length. They postulated that this nitrogen occupies the area corresponding to C(4) of the steroid, where there is evidence of an extrahydrophobic pocket. On the basis of the same postulate, we could envisage that the amino group also occupies the entrance of the area corresponding to the extrahydrophobic pocket.

Several studies have been carried out by other groups on human aromatase models [31–33]. These models, with mutation studies, revealed the importance of several residues for human aromatase [15] and particulary the role of D309, T310, K473 or H475 in the catalytic mechanism. We used this model to try to explain our results and particulary the differences in behaviour of **19** between human and equine aromatases. It could be interesting to obtain new information on the residues involved in the binding site.

In the Prosa program, as described in a recent publication [15], the model seems to exhibit a poor quality in the 150–250 region. However, we could try to collect some information on this model. The model of equine aromatase was then derived taking into account the slightly different primary structure [16]. To explain the differences of activity and behaviour of **19** towards the human and equine aromatases, we

Table II. Kinetic values of inhibitions of human and equine aromatases by indane derivatives and 4-OHA. K_m values with androstenedione were 13 and 6 nM for the human and equine enzymes respectively.

Compound	Human		Equine	
	K_i (nM)	K_i/K_m	K_i (nM)	K_i/K_m
19	86.2 ± 7.8	6.7 ± 0.6	577.7 ± 36.9	100.0 ± 6.4
21	219.5 ± 28.5	17.0 ± 2.2	539.7 ± 53.9	93.4 ± 9.3
22	88.9 ± 4.6	6.9 ± 0.4	120.5 ± 2.1	20.9 ± 0.4
4-OHA	20.2 ± 8.8	1.6 ± 0.7	6.3 ± 0.0	1.1 ± 0.0

provide two explanations. One explanation could be a possible disulfide bond between C320–C467 for equine aromatase (there is no disulfide bond in human aromatase which has F320 instead of C320). This disulfide bond with C320 on helix I (*figure 12*) could lead to a difference of conformation of the binding pocket between human and equine aromatases.

The other explanation could be a difference of aminoacid residues, at the level of the binding site, between human and equine aromatases. Indeed, a type II-spectrum was observed for human enzyme with **19** and a type I-spectrum for the equine one. Previously, an hypothesis was made regarding a possible disposition of the aminogroup of **19** at the entrance of the extrahydrophobic pocket. This extrahydrophobic pocket was supposed to be formed by a gap between the loop K473–L477 and helix B'. In this position, the aminogroup of **19** is close to D309. Near D309, presence of H475 and K473 was observed. This complexation of D309 with H475 and/or K473 could disfavor the interaction between D309 and the aminogroup of **19**, and could thus allow this compound to get close to the heme (*figure 12* and *13*). At the opposite side, in equine aromatase, H475 is replaced by N475 and this could lead to the formation of an 'acidic' pocket with D309, N475 and D476. In this case, the aminogroup of **19** could interact with this pocket leading to a different disposition of **19** in the active site (*figure 14*). The distance between the pyridyl group of **19** and iron could increase by more than 3 Å. This new position could explain the differences of spectrum and activity between the two enzymes. This hypothesis could be confirmed by the fact that compound **22**, without amino group, has a type II-spectrum for the two enzymes and a low difference of activity with an IC_{50} of 5.2 ± 2.7 μM for human aromatase and of 7.3 ± 1.8 μM for equine aromatase. Another explanation can also be proposed. The coordination of the pyridyl group to the iron atom is stronger compared to the hydrogen bound in the active site. The type I spectrum observed for **19** with the equine enzyme could be thus due to an adverse steric or electrostatic interaction with a surrounding residue, which could lead to a modification of the heme chelating binding mode. Site directed mutagenesis studies are now in progress to ascertain the binding site conformation of this crucial enzyme.

6. Conclusion

Among twelve molecules tested in this screening program, we have demonstrated that two molecules, compounds **19** (MR 20814) and **21** (MR 20818), were good inhibitors of human aromatase in comparison to **22** and 4-OHA, used as controls, whereas they weakly inhibited the equine enzyme. These differences are very interesting and shed a new light on the conformation of the active site in mammalian aromatase. This will in turn allow development of new more potent human aromatase inhibitors, which will provide also a better understanding of the active site of aromatase and the position of inhibitors within the enzyme (see molecular modelling study).

7. Experimental protocols

7.1. Materials

All chemical products were obtained from Sigma (St Quentin Fallavier, France), [1β,2β-^{3}H]-androstenedione from Dupont NEN (Les Ulis, France), Coomassie brilliant blue G-250 dye from BioRad (Ivry/Seine, France), and solvents from Carlo Erba (Val de Reuil, France) and sds (Peypin, France).

7.2. Preparation of microsomes

Human placental and equine testicular microsomes were prepared as described previously [19]. In each instance we took the tissue presenting high specific aromatase activity. Fresh

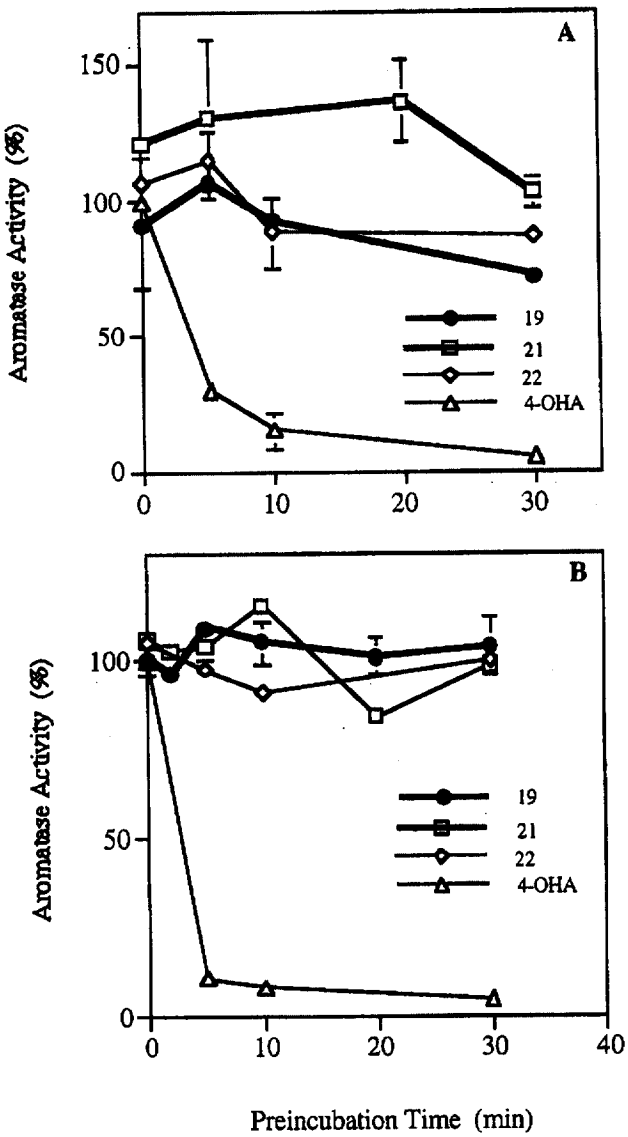

Figure 6. Effects of preincubation times of different compounds on human (A) and equine (B) aromatase activities in comparison with 4-OHA. 16 μg of microsomes from human placenta (A) or equine testis (B) were incubated with 10 μM compounds **19**, **21**, **22** or 4-OHA and 60 μM NADPH,H+ at 25 °C during 0–30 min. The compound **22** and 4-OHA were used as controls. Incubations were stopped by adding a charcoal/dextran mixture (2%:1%) and after centrifugation, aromatase activity was assayed with 300 μL of the aqueous phase. Results are expressed as % to a standard control which was incubated with NADPH,H+ and without inhibitor and are the mean of triplicate values ± SD. Compounds **19**, **21** and **22** do not appear to be inactivators.

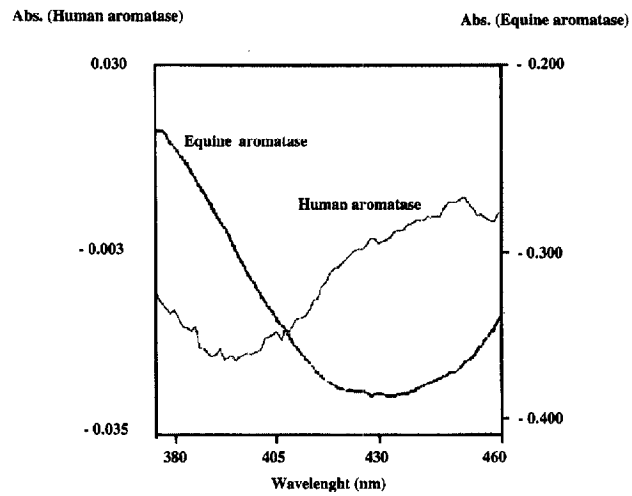

Figure 7. Spectral studies of interactions between compound **19** and the active sites of human and equine aromatases. Absorbance from 350 to 500 nm of microsomal proteins (1.5 mg) with 100 μM of compound **19** was measured at 37 °C. The spectra of the microsomes alone and of compound **19** alone were subtracted from the spectrum measured during the incubation between microsomes and the molecule. Results are representative from one of six experiments showing similar profiles.

tissue washed with 0.50 M KCl was first homogenized in 50 mM phosphate buffer pH 7.5 containing 0.25 M sucrose, 1 mM DTT, and 4 μM androstenedione in order to preserve the enzyme active site and then centrifuged at 20 000 *g*. The supernatant was further ultracentrifuged at 100 000 *g*. The final pellet was dissolved in the same buffer containing 20% glycerol, 1 mM DTT, 0.2 mM EDTA–4 Na, 4 μM androstenedione, and stored at –80 °C until use. Protein concentration was evaluated according to Bradford [34] using bovine serum albumin as standard, and Coomassie brilliant blue as dye-reagent.

7.3. Inhibition studies

Aromatase activity was evaluated by measuring ^3H_2O released from 200 nM [1β,2β-^{3}H]-androstenedione (a 2 μM substrate solution was prepared by adding 3.5 nmol of tritiated androstenedione, specific activity 1554 GBq/mmol, to 76.5 nmol nonradioactive androstenedione in 40 mL final volum of ethanol) at 37 °C during 15 min according to Thompson and Siiteri [35] in the presence of various inhibitors from 0 to 15 μM. Reactions with microsomes (16 and 20 μg of human and equine microsomal proteins respectively for determination of IC_{50} values) were initiated by adding 60 μM NADPH,H+ to a final volume of 0.5 mL and stopped by adding 1 mL of chloroform. Steroids were then extracted by incubation with a charcoal/dextran solution (7%:1.5%) and the radioactivity of the aqueous phase was measured as previously described [19]. Control incubation was realized by incubating

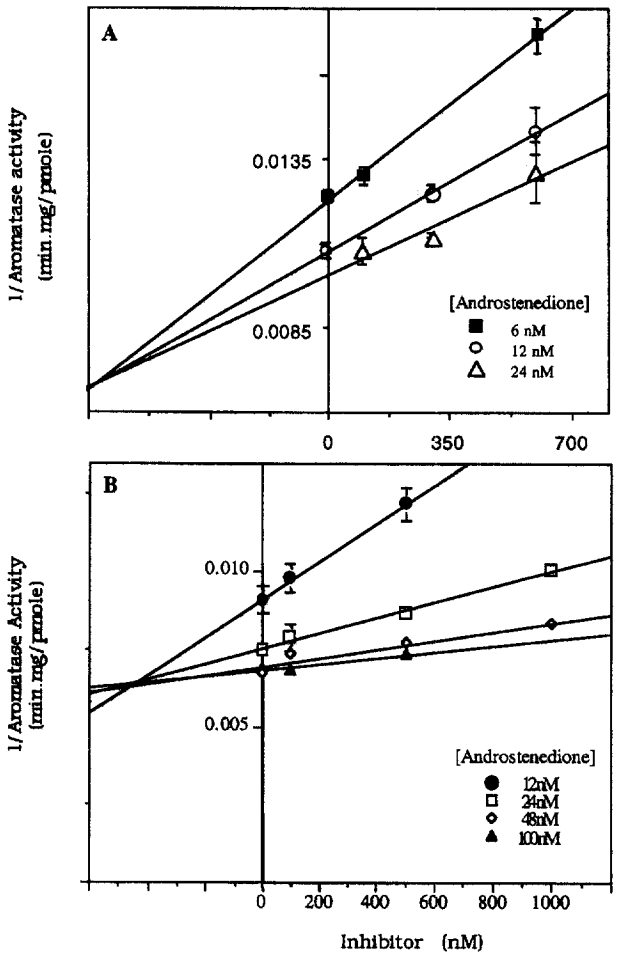

Figure 8. Dixon representation of kinetic inhibitions with **19** (A) and **21** (B) on equine aromatase. A: testicular microsomes (4 μg) were incubated with **6** to 24 nM [1β,2β-^{3}H] androstenedione and with 0 to 600 nM of compound **19** at 37 °C during 8 min. B: testicular microsomes (4 μg) were incubated with **12** to 100 nM [1β,2β-^{3}H] androstenedione and with 0 to 1000 nM of compound **21** at 37 °C during 8 min. Results are expressed as pmol estrogen formed/min mg microsomal proteins and are the mean of triplicate values ± SD.

microsomes, substrate and inhibitors without NADPH,H+ under the same conditions. The results were the mean of triplicate experiments ± SD and were expressed as pmol estrogen formed/min.mg microsomal proteins.

7.4. Kinetic studies

Concentration range for inhibitors and substrate were respectively 0–1000 and 6–102 nM. Aromatase activity was evaluated by incubating 4 μg of microsomal protein with

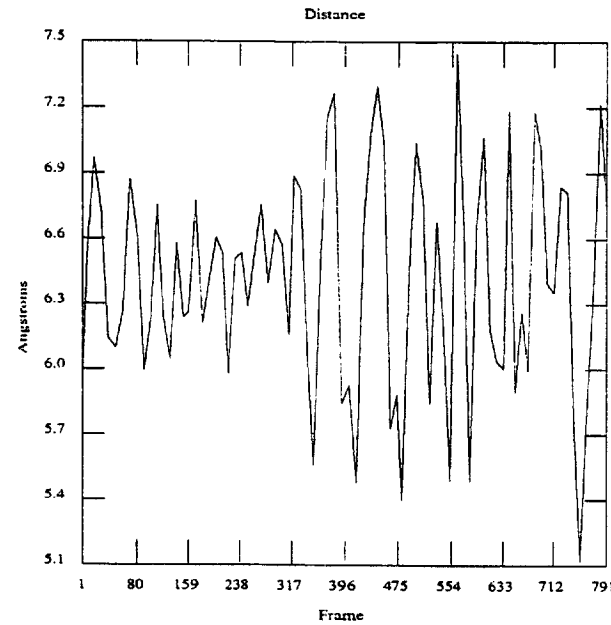

Figure 9. Evolution of the distance between oxygen and nitrogen (pyridin group) atoms during the simulation for compound **19** (see experimental protocols).

substrate and various inhibitors at 37 °C during 10 min for human aromatase or 8 min for the equine enzyme (these times have been determined to evaluate aromatase activity at the exponential portion of the Michaelis–Menten plot). K_m and K_i values were determined graphically by using respectively Lineweaver–Burk and Dixon representations.

7.5. Inactivation studies

Inactivation studies were carried out on 16 μg of microsomal proteins by testing different incubation times (0 to 30 min) at 25 °C with 10 μM inhibitors and 60 μM NADPH,H+ in 0.1 M Na–phosphate buffer, pH 7.5, containing 0.5 M sucrose as previously described [22]. Incubations were stopped by adding a charcoal/dextran mixture (2%:1%) and after centrifugation, aromatase activity was assayed with 300 μL of the aqueous phase and labelled androstenedione as described above.

7.6. Spectral studies

Absorbance of microsomal proteins (1.5 mg) in 1.5 mL of 50 mM Tris-Maleate, pH 7.4, was measured with a KONTRON-UVIKON 860 spectrophotometer. Difference absorption spectra were recorded at 37 °C over 350–500 nm after addition of 100 μM of each inhibitor diluted in ethanol (16 μL). The spectrum of ethanol was comparable to the baseline (350–500 nm). The spectra of the microsomes alone and of the molecule alone were subtracted from the spectrum of the incubation of microsomes with the molecule.

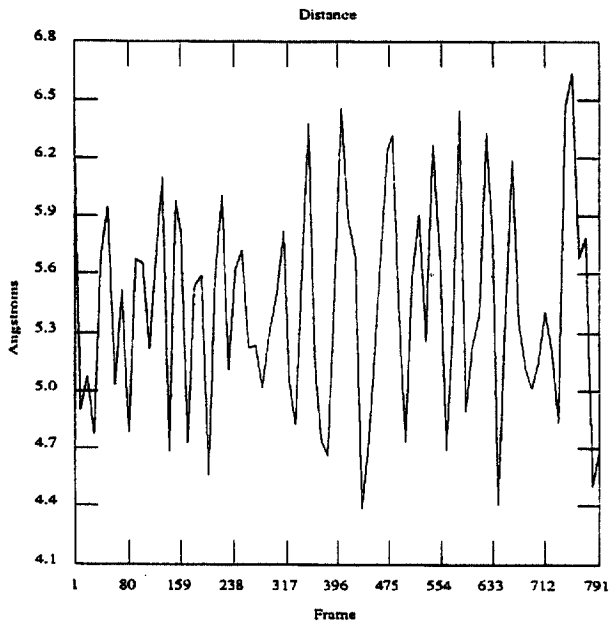

Figure 10. Evolution of the distance between the two nitrogen atoms (see *figure 11*) during the simulation for compound **19** (see Experimental protocols).

7.7. Molecular modelling

The molecular dynamic calculations were run by using the semi-empirical program MNDO94 (UNICHEM version 3.0, Cray research) on a CRAY J916. The forces on the particles are computed by calculating the negative gradient of the energy. The atomic motion is simulated by integrating the classical Newtonian equation using these forces. The gradients are computed analytically to increase speed and accuracy. The simulations were carried out firstly during 20 picoseconds and then 50 picoseconds at 300 K with a time step of 1 femtosecond. The velocities were rescaled every 100 steps. A Maxwell Boltzman distribution was applied for the initial velocities. AM1 was chosen as Hamiltonian. A microcanonical ensemble (constant energy) molecular dynamic simulation was performed. The total energy less atomic energy during the simulation was –146.3 eV ± 0.14 eV with a kinetic energy of 1.08 eV ± 0.10 eV.

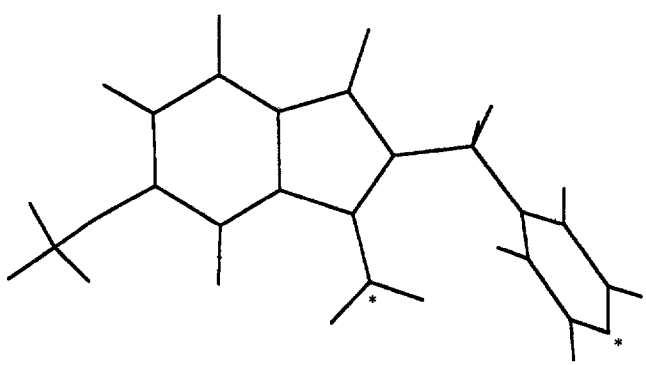

Figure 11. One conformer of compound **19** obtained during the simulation in a conformation close to compound **22**. Nitrogen atoms are indicated by asterisks.

A model of human aromatase was built in our laboratory following the recent work of Graham–Lorence et al. [33]. The initial alignment of cytochrome P450BM3 and aromatase was taken with the alignment of the previous work. Main chain coordinates for the core regions were taken from the cytochrome P450BM3 structure. Main chain coordinates for the loops were taken from a loop data base search. Refinement of the structure involved energy minimizations using AMBER 4.0 [36]. The final structure was analyzed with Procheck [37] and Prosa program [38].

7.8. Chemistry

General methods: Melting points were taken on a Köfler bank and are uncorrected. IR spectra were recorded on a Mattson 1000 FTIR apparatus and only noteworthy absorptions (reciprocal centimeters) are listed. NMR spectra were recorded on a Jeol Lambda 400 spectrometer in DMSO-d_6 solution using TMS as an internal standard. Chemical shift is reported in ppm downfield (δ) from TMS.

7.8.1. (E)-2-Arylmethylene-3-trifluoroacetylaminoindan-1-ones ***10–16***

General method: A 5 N aqueous sodium hydroxide solution (3 mL) was added to a solution of 3-trifluoroacetylaminoindan-1-one **7–9** (0.006 mol) in ethanol (4 mL). Arylcarboxaldehyde (0.009 mol) was then added to the reaction mixture which was stirred at room temperature for 2 h. 2-Arylmethylene-3-trifluoroacetylaminoindan-1-ones **10–16** were precipitated from the solution by addition of a 10% aqueous hydrochloric acid solution. The precipitates were filtered, washed with water (15 mL), dried and recrystallized to give the *E*-form of **10–16**

7.8.2. (E)-2-(3-Methoxybenzylidene)-3-trifluoroacetylamino-5,6,7-trimethoxyindan-1-one ***10***

Colorless crystals (62%); m.p. 192 °C (ether); IR (KBr) 3250 (NH), 1705, 1680 (CO); ^{1}H NMR (DMSO-d_6) 9.96 (1H, d, J = 6 Hz, NH), 7.50 (1H, s, vinyl-H), 7.33 (1H, t, J = 8.0 Hz, H-5'), 7.16 (2H, d, J = 2.9 Hz, H-2' and H-6'), 7.00 (1H, d, J = 8.3 Hz, H-4'), 6.84 (1H, s, H-4), 6.48 (1H, d, J = 6 Hz, H-3), 3.98 (3H, s, OCH_3), 3.90 (3H, s, OCH_3), 3.78 (3H, s, OCH_3), 3.77 (3H, s, OCH_3); Found: C, 58.81; H, 4.29; N, 3.07; Calc. for $C_{22}H_{20}NO_6F_3$: C, 58.54, H; 4.47; N, 3.10.

7.8.3. (E)-2-(3,4-Dimethoxybenzylidene)-5-methoxy-3-trifluoroacetylaminoindan-1-one ***11***

Yellow crystals (62%); m.p. 219 °C (propan-2-ol/ethanol 80:20); IR (KBr) 3210 (NH), 1705, 1675 (CO); ^{1}H NMR (DMSO-d_6) 10.08 (1H, br s, NH), 7.78 (1H, d, J = 7.8 Hz, H-7), 7.55 (1H, s, vinyl-H), 7.10 (5H, m, H-6, H-4, H-2', H-5' and H-6'), 6.54 (1H, d, J = 6 Hz, H-3), 3.88 (3H, s, OCH_3), 3.82 (3H, s, OCH_3), 3.79 (3H, s, OCH_3); Found: C, 59.71; H, 4.31; N, 3.19; Calc. for $C_{21}H_{18}NO_5F_3$: C, 59.86, H; 4.31; N, 3.32.

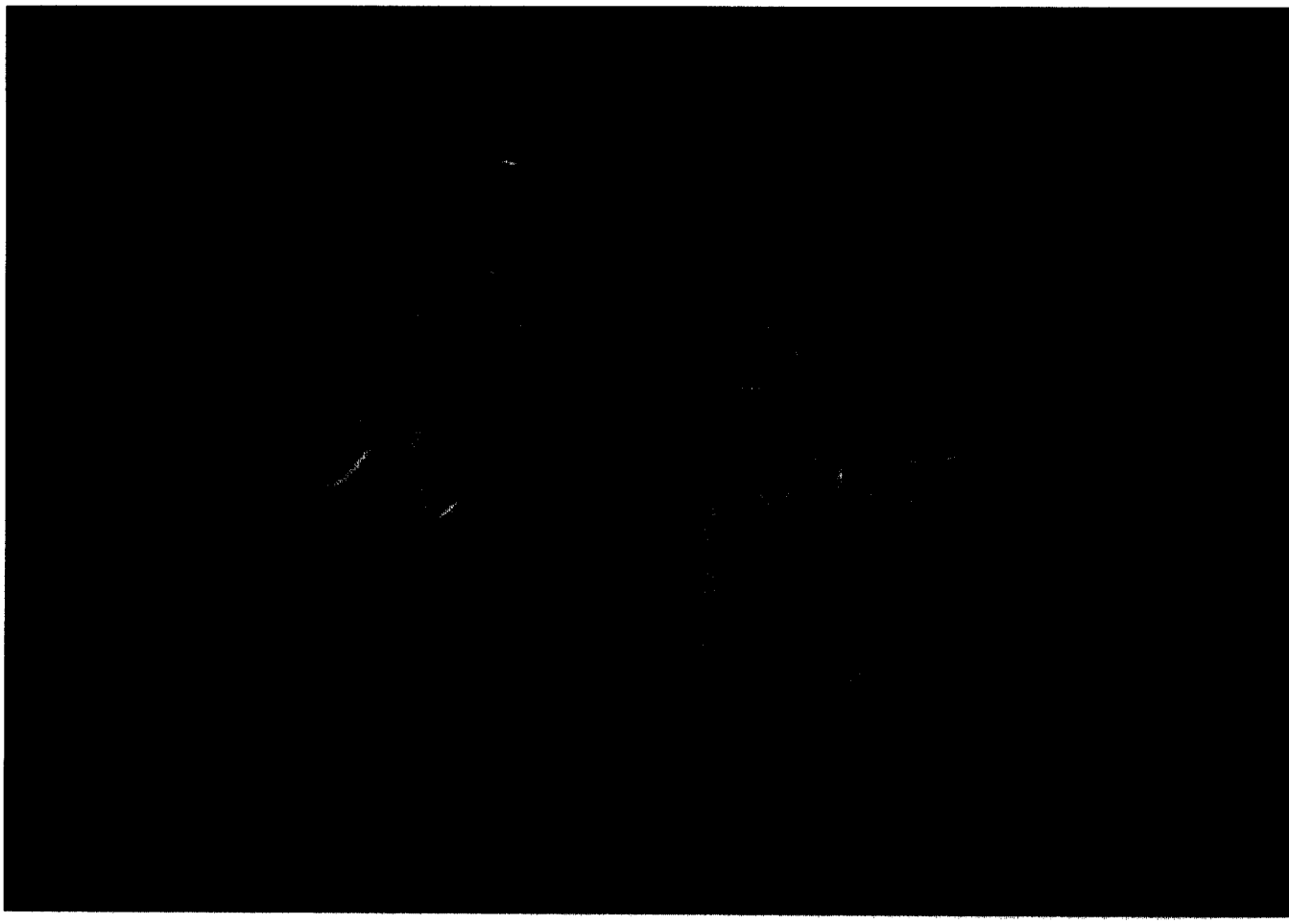

Figure 12. Model structure of human $P450_{arom}$ with compound **19** in the active site. The entrance of the substrate access channel is indicated in purple. The area corresponding to D309, K473 and H475–D476 is indicated in blue, while the positions of residues 320 and 467 corresponding to the possible disulfide bond for equine aromatase are indicated in pink. Compound **19** is represented in the center over the developed heme structure. The representation includes residues after the membrane-spanning domain from 69 to 496.

7.8.4. (E)-5,6-Dimethoxy-2-(3,4-dimethoxybenzylidene)-3-trifluoroacetylaminoindan-1-one ***12***

Yellow crystals (47%); m.p. > 260 °C (ethanol); IR (KBr) 3280 (NH), 1700, 1680 (CO); ^{1}H NMR (DMSO-d_6) 10.02 (1H, br s, NH), 7.51 (1H, s, vinyl-H), 7.2 (3H, m, H-7, H-2' and H-5'), 7.01 (2H, m, H-4 and H-6'), 6.46 (1H, m, H-3), 3.87 (6H, s, 2 OCH_3), 3.79 (3H, s, OCH_3), 3.81 (3H, s, OCH_3); Found: C, 58.80; H, 4.41; N, 2.98; Calc. for $C_{22}H_{20}NO_6F_3$: C, 58.54, H; 4.47; N, 3.10.

7.8.5. (E)-3-Trifluoroacetylamino-3,4,5-trimethoxy-2-(3,4,5-trimethoxybenzyliden)indan-1-one ***13***

Yellow crystals (65%); m.p. 190 °C (ethanol); IR (KBr) 3200 (NH), 1700, 1680 (CO); ^{1}H NMR (DMSO-d_6) 10.00 (1H, d, J = 6 Hz, NH), 7.49 (1H, s, vinyl-H), 6.92 (2H, m, H-5' and H-6'), 6.85 (1H, s, H-4), 6.51 (1H, d, J = 6 Hz, H-3), 3.98 (3H, s, OCH_3), 3.90 (3H, s, OCH_3), 3.81 (3H, s, OCH_3), 3.77 (3H, s, OCH_3), 3.69 (3H, s, OCH_3); Found: C, 56.37; H, 4.56; N, 2.61; Calc. for $C_{24}H_{24}NO_8F_3$: C, 56.36, H; 4.73; N, 2.74.

7.8.6. (E)-5-Methoxy-2-(pyridin-3-ylmethylene)-3-trifluoroacetylaminoindan-1-one ***14***

Colorless crystals (75%); m.p. 212 °C (propan-2-ol); IR (KBr) 3160 (NH), 1690, 1625 (CO); ^{1}H NMR (DMSO-d_6) 10.04 (1H, br s, NH), 8.82 (1H, s, H-2'), 8.57 (1H, m, H-6'), 7.96 (1H, m, H-4'), 7.80 (1H, d, J = 7.8 Hz, H-7), 7.61 (1H, s, vinyl-H), 7.44 (1H, m, H-5'), 7.18 (1H, d, J = 7.8 Hz, H-6), 7.00 (1H, s, H-4), 6.58 (1H, s, H-3), 3.91 (3H, s, OCH_3); ^{13}C NMR (DMSO-d_6) 189.10 (C-1), 165.61 (C-5), 156.73 (CO), 152.92 (C-2'), 151.39 (C-6'), 150.19 (C-7a), 143.86 (C-3'), 136.80 (C-4'), 130.84 (C-a), 130.11 (C-3a), 129.33 (C-2), 125.52 (C-7), 123.34 (C-5'), 117.28 (C-6), 115.79 (CF_3),

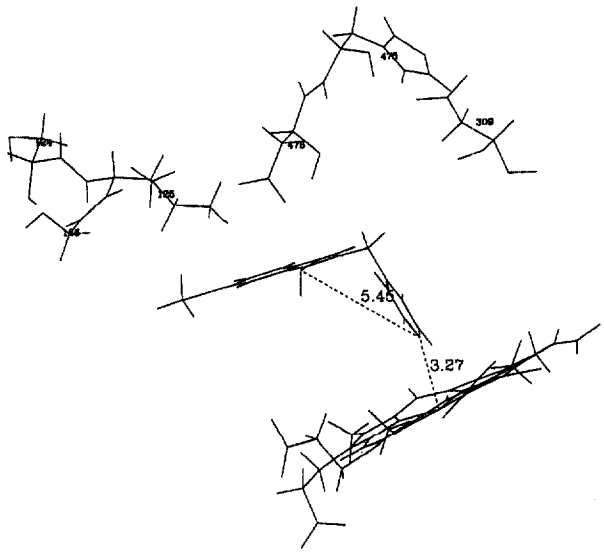

Figure 13. Hypothetical position of compound **19** in the active site of human $P450_{arom}$. The distances between the nitrogen of the pyridin group and the iron of heme and between the two nitrogens of compound **19** are indicated in Å. Some of the positioned residues (124 to 309) are indicated.

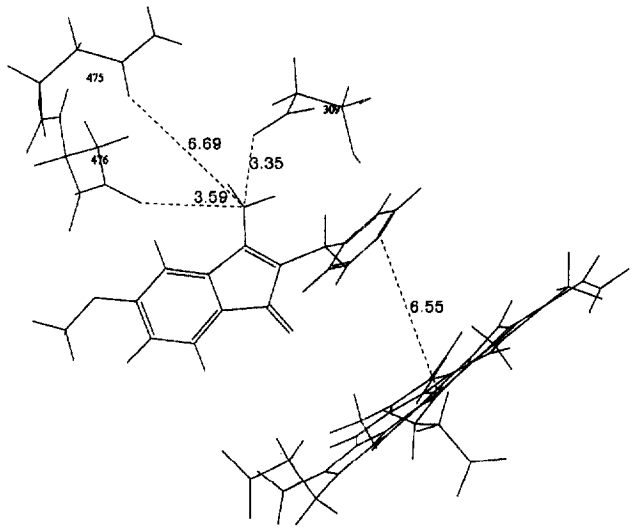

Figure 14. Hypothetical position of compound **19** in the active site of equine $P450_{arom}$. The distances between compound **19**, the 'acidic pocket' and the heme group are indicated in Å. Some residues (309, 475, 476) are positioned.

108.79 (C-4), 56.05 (OCH_3), 48.90 (C-3); Found: C, 59.39; H, 3.58; N, 7.68; Calc. for $C_{18}H_{13}N_2O_3F_3$: C, 59.67, H; 3.62; N, 7.73.

7.8.7. (E)-5,6-Dimethoxy-2-(pyridin-3-ylmethylene)-3-trifluoroacetylaminoindan-1-one ***15***

Yellow crystals (64%); m.p. > 260 °C (propan-2-ol/ethanol 60:40); IR (KBr) 3150 (NH), 1695, 1630 (CO); ^{1}H NMR (DMSO-d_6) 9.99 (1H, d, J = 6.3 Hz, NH), 8.81 (1H, s, H-2'), 8.60 (1H, d, J = 4.4 Hz, H-6'), 7.94 (1H, d, J = 7.8 Hz, H-4'), 7.58 (1H, s, vinyl-H), 7.46 (1H, dd, J = 7.8 Hz, J = 4.4 Hz, H-5'), 7.27 (1H, s, H-7), 7.00 (1H, s, H-4), 6.43 (1H, m, H-3), 3.91 (3H, s, OCH_3), 3.88 (3H, s, OCH_3); Found: C, 57.98; H, 3.72; N, 6.95; Calc. for $C_{19}H_{15}N_2O_4F_3$: C, 58.17, H; 3.85; N, 7.14.

7.8.8. (E)-5,6-Dimethoxy-2-(pyridin-4-ylmethylene)-3-trifluoroacetylaminoindan-1-one ***16***

Yellow crystals (65%); m.p. > 260 °C (propan-2-ol/methanol 60:40); IR (KBr) 3150 (NH), 1700, 1685 (CO); ^{1}H NMR (DMSO-d_6) 9.96 (1H, br s, NH), 8.61 (2H, d, J = 4.9 Hz, H-2' and H-6'), 7.52 (3H, m, H-3', H-4' and vinyl-H), 7.30 (1H, s, H-7), 7.01 (1H, s, H-4), 6.55 (1H, m, H-3), 3.90 (3H, s, OCH_3), 3.88 (3H, s, OCH_3); Found: C, 57.91; H, 3.91; N, 7.17; Calc. for $C_{19}H_{15}N_2O_4F_3$: C, 58.17, H; 3.85; N, 7.14.

7.8.9. 3-Amino-2-arylmethylinden-1-ones ***17–21***

General method: A 5 N aqueous sodium hydroxide solution (3 mL) was added to a solution of 3-trifluoroacetylaminoindan-1-one **7–9** (0.006 mol) in ethanol (4 mL). Arylcarboxaldehyde (0.009 mol) was then added to the reaction mixture which was stirred at room temperature for 24 h. Addition of water (100 mL) gave a precipitate which was filtered, washed with water (15 mL), dried and recrystallized to give **17–21**.

7.8.10. 3-Amino-5-methoxy-2-(pyridin-3-ylmethyl)inden-1-one ***17***

Yellow crystals (40%); m.p. 220 °C (propan-2-ol); IR (KBr) 3360–3300 (NH_2), 1640 (CO); ^{1}H NMR (DMSO-d_6) 8.47 (1H, s, H-2'), 8.32 (1H, m, H-6'), 7.59 (3H, m, NH_2 and H-4'), 7.22 (2H, m, H-4 and H-5'), 7.12 (1H, d, J = 7.8 Hz, H-7), 6.73 (1H, d, J = 7.8 Hz, H-6), 3.79 (3H, s, OCH_3), 3.50 (2H, s, CH_2); Found: C, 71.73; H, 5.58; N, 10.33; Calc. for $C_{16}H_{14}N_2O_2$: C, 72.17, H; 5.30; N, 10.52.

7.8.11. 3-Amino-2-(pyridin-3-ylmethyl)-5,6,7-trimethoxyinden-1-one ***18***

Yellow crystals (60%); m.p. 220 °C (ether); IR (KBr) 3360–3300 (NH_2), 1640 (CO); ^{1}H NMR (DMSO-d_6) 8.46 (1H, s, H-2'), 8.36 (1H, m, H-6'), 7.55 (3H, m, NH_2 and H-4'), 7.24 (2H, m, H-4 and H-5'), 3.90 (3H, s, OCH_3), 3.83 (3H, s, OCH_3), 3.67 (3H, s, OCH_3), 3.45 (2H, s, CH_2); Found: C, 66.18; H, 5.61; N, 8.63; Calc. for $C_{18}H_{18}N_2O_4$: C, 66.25, H; 5.56; N, 8.58.

7.8.12. 3-Amino-5-methoxy-2-(pyridin-4-ylmethyl)inden-1-one ***19***

Orange crystals (56%); m.p. 218 °C (ether); IR (KBr) 3360–3300 (NH_2), 1640 (CO); ^{1}H NMR ($CDCl_3$) 8.40 (2H, m, H-2' and H-6'), 7.74 (2H, s, NH_2), 7.23 (3H, m, H-4, H-3' and H-5'), 7.14 (1H, d, J = 7.8 Hz, H-7), 6.75 (1H, dd, J = 7.8 Hz, J = 2 Hz, H-6), 3.79 (3H, s, OCH_3), 3.61 (2H, s, CH_2);

^{13}C NMR ($CDCl_3$) 191.25 (C-1), 162.45 (C-5), 161.58 (C-4'), 150.66 (C-7a), 149.69 (C-2' and C-6'), 141.50 (C-2), 127.83 (C-3a), 124.04 (C-4), 120.72 (C-7), 111.78 (C-6), 107.77 (C-3' and C-5'), 102.24 (C-3), 56.00 (OCH_3), 26.36 (CH_2); MS *m/e* 267 (M, 22%), 266 (M-H, 100%); Found: C, 71.93; H, 5.21; N, 10.24; Calc. for $C_{16}H_{14}N_2O_2$: C, 72.17, H; 5.30; N, 10.52.

7.8.13. 3-Amino-5,6-dimethoxy-2-(pyridin-4-ylmethyl)inden-1-one ***20***

Red crystals (56%); m.p. 212 °C (propan-2-ol); IR (KBr) 3400–3200 (NH_2), 1640 (CO); ^1H NMR (DMSO-d_6) 8.40 (2H, d, J = 5.2 Hz, H-2' and H-6'), 7.66 (2H, s, NH_2), 7.38 (1H, s, H-6), 7.25 (2H, m, H-3' and H-5'), 6.90 (1H, s, H-4), 3.80 (3H, s, OCH_3), 3.78 (3H, s, OCH_3), 3.51 (2H, s, CH_2); Found: C, 69.01; H, 5.32; N, 9.48; Calc. for $C_{17}H_{16}N_2O_3$: C, 68.91, H; 5.40; N, 9.45.

7.8.14. 3-Amino-2-(pyridin-4-ylmethyl)-5,6,7-trimethoxyinden-1-one ***21***

Orange crystals (50%); m.p. 218 °C (ether); IR (KBr) 3360–3300 (NH_2), 1640 (CO); ^1H NMR (DMSO-d_6) 8.39 (2H, m, H-2' and H-6'), 7.59 (2H, s, NH_2), 7.26 (1H, s, H-4), 7.20 (2H, m, H-3' and H-5'), 3.90 (3H, s, OCH_3), 3.84 (3H, s, OCH_3), 3.67 (3H, s, OCH_3), 3.46 (2H, s, CH_2); Found: C, 66.32; H, 5.59; N, 8.61; Calc. for $C_{18}H_{18}N_2O_4$: C, 66.25, H; 5.56; N, 8.58.

Acknowledgements

This work was initiated and developed through a grant from the Ligue Nationale Contre Le Cancer for the biological study (Comité de la Manche), and recently supported by the Ligue Nationale Contre Le Cancer, Comité du Calvados, for the chemical syntheses. We wish to thank the Conseil Général du Calvados for financial supports on equine studies. We are grateful to Dr. Bruno Plainfossé for providing horse tissues and M.-J. Simon for technical assistance. P. Auvray is recipient of a studentship from Ligue Nationalè Contre Le Cancer (Comité de la Manche) and S. Moslemi is recipient of a fellowship from the Fondation pour la Recherche Médicale (Paris, France).

References

[1] Simpson E.R., Mahendroo M.S., Means G.D., Kilgore M.W., Hinshelwood M.M., Graham-Lorence S., Amarneh B., Ito Y., Fisher C.R., Dodson Michael M., Mendelson C.R., Bulun S.E., Endocr. Rev. 15 (1994) 342–355.
[2] Sergejew T., Hartmann R.W., J. Enz. Inhib. 8 (1994) 113–122.
[3] Hartmann R.W., Bayer H., Grün G., J. Med. Chem. 37 (1994) 1275–1281.
[4] Banting L., Progr. Med. Chem. 33 (1996) 147–184.
[5] Griffiths C.T., Hall T.C., Saba Z., Barlow J.J., Nevinny H.B., Cancer 32 (1973) 31–37.
[6] Brodie A.M., J. Steroid. Biochem. Mol. Biol. 40 (1991) 255–261.
[7] Trunet P.F., Bhatnagar A.S., Chaudri H.A., Hornberger U., Acta Oncol. 35 (1996) 15–18.
[8] Wouters W., Snoeck E., De Coster R., Breast Cancer Res. Treat. 30 (1994) 89–94.
[9] Dukes M., Edwards P.N., Large M., Smith I.K., Boyle T., J. Steroid. Biochem. Mol. Biol. 58 (1996) 439–445.
[10] Howell A., Downey S., Anderson E., Eur. J. Cancer 32A (1996) 576–588.
[11] Miller W.R., British J. Cancer 73 (1996) 415–417.
[12] Poulos T.L., Finzel B.C., Howard A.J., J. Mol. Biol. 195 (1987) 687–700.
[13] Ravichandran K.G., Boddupalli S.S., Hasemann C.A., Peterson J.A., Deisenhofer J., Science 261 (1993) 731–736.
[14] Hasemann C.A., Ravichandran K.G., Peterson J.A., Deisenhofer J., J. Mol. Biol. 236 (1994) 1169–1185.
[15] Kao Y.C., Cam L.L., Laughton C.A., Zhou D., Chen S., Cancer Res. 56 (1996) 3451–3460.
[16] Tomilin A., Komarova E., Moslemi S., Auvray P., Sourdaine P., Drosdowsky M.A., Séralini G.E., IVth International Aromatase Conference, Tahoe-City, California, 1996, Abst. no. A22.
[17] Gaillard J.L., Silberzahn P., J. Biol. Chem. 262 (1987) 5717–5722.
[18] Gaillard J.L., Comp. Biochem. Physiol. 100B (1991) 107–115.
[19] Dintinger T., Gaillard J.L., Zwain I., Bouhamidi R., Silberzahn P., J. Steroid. Biochem. 32 (1989) 537–544.
[20] Almadhidi J., Séralini G.E., Fresnel J., Silberzahn P., Gaillard J.L., J. Histochem. Cytochem. 43 (1995) 571–577.
[21] Almadhidi J., Moslemi S., Drosdowsky M.A., Séralini G.E., J. Steroid. Biochem. Molec. Biol. 59 (1996) 55–61.
[22] Moslemi S., Séralini G.E., J. Enz. Inhib. 12 (1997) 241–254.
[23] Moslemi S., Vibet A., Papadopoulos V., Camoin L., Silberzahn P., Gaillard J.L., Comp. Biochem. Physiol. 118B (1997) 217–227.
[24] Moslemi S., Dintinger T., Dehennin L., Silberzahn P., Gaillard J.L., Eur. J. Biochem. 214 (1993) 569–576.
[25] Dallemagne P., Rault S., Pilo J.C., Foloppe M.P., Robba M., Tetrahedron Lett. 44 (1991) 6327–6328.
[26] Bayer H., Batz C., Hartmann R.W., Mannschreck A., J. Med. Chem. 34 (1991) 2685–2691.
[27] Brodie A.M.H., Garett W.M., Hendrickson J.R., Tsai-Morris C.H., Marcotte P.A., Robinson C.H., Steroids 38 (1981) 693–702.
[28] Schenkman J.B., Biochemistry 9 (1970) 2081–2091.
[29] Moslemi S., Auvray P., Sourdaine P., Drosdowsky M.A., Séralini G.E., Ann. N. Y. Acad. Sci. 839 (1998) 576–577.
[30] Laughton C.A., Mckenna R., Neidle S., Jarman M., McCague R., J. Med. Chem. 33 (1990) 2673–2679.
[31] Furet P., Batzl C., Bhatnagar A., Francotte E., Rihs G., Lang M., J. Med. Chem. 36 (1993) 1393–1400.
[32] Laughton C.A., Zvelebil M.J., Neidle S.A., J. Steroid. Biochem. Mol. Biol. 44 (1993) 399–407.
[33] Graham-Lorence S., Amarneh B., White R.E., Peterson J.A., Simpson E.R., Protein Sci. 4 (1995) 1065–1080.
[34] Bradford M., Anal. Biochem. 72 (1976) 248–254.
[35] Thompson E.A., Siiteri P.K., J. Biol. Chem. 249 (1974) 5373–5378.
[36] Pearlman D.A., Case D.A., Caldwell J.C., Seobe G.L., Chandra Singh U., Weiner P., Kollman P.A., AMBER 4.0, University of California, San Francisco, CA, 1991.
[37] Laskowski R.A., MacArthur M.W., Moss D.S., Thorton J.M., J. Appl. Cryst. 26 (1993) 283–291.
[38] Sippl M.J., Proteins 17 (1993) 355–362.